PHYSICAL REVIEW B VOLUME 14, NUMBER 8 15 OCTOBER 1976

Electronic structure of palladium and its relation to uv spectroscopy

N. E. Christensen
Physics Laboratory I, The Technical University of Denmark, DK-2800 Lyngby, Denmark
(Received 23 February 1976)

The electronic-energy-band structure of palladium has been calculated by means of the relativistic augmented-plane-wave method covering energies up to 30 eV above the Fermi level. The optical interband transitions producing structure in the dielectric function up to photon energies of 25 eV have been identified. Also the photoemission spectra for polycrystalline samples can be interpreted in terms of the present band model, and the regions in $\vec{k}$ space contributing to various elements of structure have been traced out.

I. INTRODUCTION

Ab initio calculations of the electronic band structure of palladium have been reported previously by Mueller *et al.*[1] and by Andersen.[2] Whereas the work of Ref. 1 was based on the nonrelativistic augmented plane wave (APW) method in conjunction with a combined interpolation scheme[3] (also including spin-orbit coupling) Andersen[2] applied the fully relativistic augmented plane wave (RAPW) method. Fermi-surface properties represented the main object of the calculations presented in Refs. 1 and 2, and thus little attention was paid to the energy bands far above the Fermi level (E_F). The aim of the present work is to examine the optical properties of Pd such as they manifest themselves in experimental recordings of absorption spectra and photoemission spectra in the ultraviolet (uv) regime. Therefore we needed to extend the previous calculations to include energy levels up to 30 eV above E_F. This was done by means of the RAPW method using the same muffin-tin potential as in Ref. 2.

Experimentally, the optical-absorption profile of Pd has been studied very extensively. In spite of the great amount of experimental results surprisingly little can be extracted about the electronic structure. The disagreement in the published optical data is slightly overwhelming, but is probably due to the difficulty in cleaning[4,5] the samples and preventing the contamination of virtually clean surfaces. Also aging effects appear to be significant. Weaver[6] recently compared several experimental results,[4,5,7-11] and further gave some interpretation in terms of combined interpolation-scheme[3,12] band-structure calculations.[13-15] Although this type of interpolation scheme can be adjusted to reproduce well the band structure in the d-band regime and a few electron volts above E_F, it fails when higher-energy levels (above 10 eV above E_F) are considered.[16] Therefore, an attempt to relate the optical experiments at photon energies exceeding ~10 eV to a band model must rely on a more exact calculation, such as obtained by the RAPW method, for instance.

Measurements of photoelectron energy spectra have been described by several authors, and some of the most definitive results are probably those presented by Janak, Eastman, and Williams[17] and by Traum and Smith.[14] The work described in Ref. 17 includes experimental photoemission spectra for photon energies ranging from 7.7 to 11.6 eV as well as theoretical calculations of the spectra within the direct transition model. The energy bands were obtained by means of the nonrelativistic Korringa-Kohn-Rostoker[18] method. The experimental work of Ref. 14 represents a part of a systematic study[13-15] of the photoemission spectra from fcc d-band metals and the relation of these spectra to band-structure models.

The main body of the present paper consists of three Secs. II–IV. The band-structure calculation is described in Sec. II. Since the present band calculation is an extension of the one obtained by Andersen,[2] the results concerning the Fermi surface which can be deduced are identical to those described in Ref. 2, and therefore they will not be considered here. The interband contribution to the imaginary part of the dielectric function is shown in Sec. III, and an attempt to interpret optical experiments from this theoretical profile and partial joint density-of-states functions is presented. Section IV contains the calculated photoemission spectra and a discussion of their relation to the experiments.

II. Pd BAND STRUCTURE

The crystal potential which was used in the present calculations is identical to the one used by Andersen.[2] It is constructed from relativistic Dirac-Slater atomic charge densities[19] calculated

for the $4d^{10}$ configuration. The lattice constant is $a = 7.3508$ a.u., the radius in the muffin-tin sphere $R_S = 2.5857$ a.u., and the Wigner-Seitz radius is $S = 2.8727$ a.u. The constant potential between the muffin-tin spheres is $V_{MTZ} = -1.0294$ Ry. We have not tried to incorporate shifts in the band structure due to non-muffin-tin effects. The neglect of these corrections is justified by the calculations by Painter *et al.*,[20] who found that the shifts in Pd were small, a few mRy, for the majority of the energy levels, the most serious corrections being 0.010 and -0.012 Ry at the *sd*-like X_1 and the *p*-like X_4, respectively. The standard RAPW calculation applied here thus follows the lines of previous calculations.[2,21]

Twelve eigenvalues were calculated at 89 $\vec{k}$ points uniformly distributed over the irreducible $\frac{1}{48}$ Brillouin zone. The results are listed in Table I, and the band structure along symmetry lines is shown in Fig. 1. Characteristic energy gaps are compared to the results obtained by Mueller *et al.*[1] in Table II. The eigenvalues were interpolated onto a finer $\vec{k}$ mesh by means of a second-order interpolation scheme,[21] and using the Gilat-Raubenheimer[22] integration procedure the density-of-states function $N(E)$ was calculated. This function is shown in Figs. 2(a) and 2(b). Critical points are indicated by the symmetry-point label and level number, the levels being counted from below in energy. The Fermi level which was found by integrating $N(E)$ is $E_F = 0.558$ Ry, and $N(E_F) = 32.1$ (states/atom)/Ry. These values agree with those obtained by Andersen[2] by means of constant-energy surface integrations.

The spin-orbit splitting ΔE_{SO} as obtained in the RAPW calculation is 0.022 Ry at $\Gamma(\Gamma'_{25} \rightarrow \Gamma_8^+ + \Gamma_7^+)$ and $X(X_5 \rightarrow X_6^+ + X_7^+)$. In fact one would expect these numbers to differ since $\Delta E_{SO} \simeq \frac{3}{2}\xi_{4d}$ at Γ and $\Delta E_{SO} \simeq \xi_{4d}$ at X. The value of ξ_{4d} evaluated at $E = E(\Gamma'_{25})$ thus becomes 0.014 Ry whereas the value at the top of the *d*-band is larger, namely 0.022 Ry. The apparent SO parameter increases when the energy is varied from the bottom to the top of the *d*-band.[2,16] The atomic spin-orbit parameter for the 4*d*-states is[23] 0.015 Ry, and thus very close to the values near the center of the *d* band.

III. OPTICAL INTERBAND TRANSITIONS

Recently Rijsenbrij and Fondse[24] concluded from a nonrelativistic Korringa-Kohn Rostoker calculation on silver, that it is not necessary to include relativistic effects when the band structure is compared to optical measurements. Apparently their results, as well as an earlier APW calculation[25] for Ag, agreed better with the majority of optical measurements, in particular, concerning the gap L_1-L'_2, than did the RAPW calculation.[26] However, this does not mean that relativistic effects should be excluded, but rather it indicates that slight corrections to the crystal potential (non-muffin-tin terms) are necessary to obtain a correct value of this gap. The fact that the RAPW results differ from the APW results in the case of silver, and thus also for Pd, by up to 1 eV definitively indicates that relativistic effects are important when the band model is checked against optical measurements where the accuracy often is ≈ 0.1 eV. Therefore, we shall here only consider the relativistic band models when comparing to optical experiments.

The partial joint density-of-states function corresponding to the initial band i and final band f is defined through

$$J_{if}(\hbar\omega) = \frac{2\Omega}{(2\pi)^3}\int d\vec{k}\,\delta(E_F(\vec{k}) - E_i(\vec{k}) - \hbar\omega) \times f(E_i(\vec{k}))[1 - f(E_f(\vec{k}))]. \quad (1)$$

This function is a measure of the number of transitions between states i and f separated in energy by $\hbar\omega$. The Fermi functions $f(E_i(\vec{k}))$ and $[1-f(E_f(\vec{k}))]$ ensure that only occupied initial states and empty final states are included. The total joint density of states $J(\hbar\omega)$ is obtained by summing over all i and f:

$$J(\hbar\omega) = \sum_{i,f} J_{if}(\hbar\omega)\,. \quad (2)$$

If the optical transition matrix elements could be considered as independent of energy and wave number, this function (2) would be proportional to the interband part of the imaginary part $\epsilon_2(\omega)$ of the dielectric function multiplied by ω^2. Experimentally the interband contribution to $\epsilon_2(\omega)$ is obtained by static reflectance measurements. Although modulation spectroscopy offers a greater opportunity to identify transitions at specific points in $\vec{k}$ space, such as critical points, no such results have been presented for Pd. We therefore must rely on static experimental ϵ_2 profiles in our interpretation and realize that critical transitions may easily be masked by a large noncritical background, which even may contain structure due to varying matrix elements.

Some of the experimental observations may be briefly summarized by quoting a few spectral positions of "structure" in the reflectivity of Pd. Duisebaeva *et al.*[7] reported structure at 0.5 eV, Lostis[10] at 1.1 eV, Johnson and Christy[11] found a change in slope at 1.4 eV, minima near 2.4 and 4.5 eV, whereas Vehse *et al.*[4] reported a minimum at 4 eV and the measurements by Yu and Spicer[5]

TABLE I. Energy eigenvalues at 89 $\vec{k}$ points as obtained by the RAPW method. The energies are measured in mRy from the muffin-tin zero ($V_{MTZ}=-1.0294$ Ry).

	$\vec{k}/\frac{\pi}{4a}$	Band 1	Band 2	Band 3	Band 4	Band 5	Band 6	Band 7	Band 8	Band 9	Band 10	Band 11	Band 12
Γ	0 0 0	43	353	353	375	472	472	1860	2150	2162	2162	2508	2800
Δ	0 1 0	57	347	356	378	464	475	1874	2104	2147	2161	2605	2732
Δ	0 2 0	96	330	372	393	445	483	1913	2015	2100	2123	2652	2669
Δ	0 3 0	152	303	393	420	432	495	1943	1967	2002	2033	2515	2657
Δ	0 4 0	198	273	419	454	457	511	1864	1882	1906	2026	2290	2730
Δ	0 5 0	203	244	478	497	513	520	1731	1750	1770	2080	2147	2860
Δ	0 6 0	185	221	525	529	553	630	1581	1635	1663	2103	2122	2947
Δ	0 7 0	168	206	543	557	580	759	1414	1553	1587	2102	2148	3219
X	0 8 0	161	201	547	570	591	825	1333	1525	1560	2106	2157	2879
Σ	1 1 0	70	345	359	381	461	473	1884	2020	2146	2215	2575	2735
	1 2 0	108	330	370	395	447	483	1905	1924	2117	2215	2517	2683
	1 3 0	163	305	382	418	443	500	1842	1905	2076	2108	2513	2623
	1 4 0	208	277	390	452	473	526	1765	1830	1955	2085	2356	2669
	1 5 0	213	250	429	493	514	580	1675	1721	1785	2119	2229	2778
	1 6 0	194	228	477	530	543	683	1573	1605	1624	2150	2179	2854
	1 7 0	177	214	514	544	571	820	1416	1523	1553	2155	2175	2858
Z	1 8 0	170	209	531	544	583	874	1332	1497	1528	2165	2170	2851
Σ	2 2 0	143	325	372	402	440	492	1817	1878	2134	2328	2352	2736
	2 3 0	192	310	369	419	437	530	1728	1818	2148	2165	2464	2636
	2 4 0	236	288	357	450	462	580	1649	1730	1979	2187	2455	2597
	2 5 0	242	266	371	489	496	657	1572	1629	1799	2209	2362	2679
	2 6 0	220	248	409	512	536	770	1501	1537	1611	2226	2327	2733
	2 7 0	201	236	445	516	568	901	1416	1460	1480	2236	2330	2749
Z	2 8 0	194	232	462	513	580	978	1330	1434	1458	2240	2336	2749
Σ	3 3 0	233	310	361	419	434	581	1631	1723	2106	2240	2385	2730
	3 4 0	270	303	338	432	458	647	1550	1621	1993	2299	2326	2715
	3 5 0	279	292	324	461	495	738	1481	1520	1831	2316	2329	2770
	3 6 0	253	281	349	480	534	859	1430	1450	1643	2335	2364	2752
	3 7 0	230	273	375	482	567	1002	1362	1392	1463	2335	2451	2680
Z	3 8 0	223	270	388	479	579	1098	1329	1342	1400	2335	2533	2603
Σ	4 4 0	286	314	333	420	473	726	1472	1512	1999	2170	2409	2684
	4 5 0	286	309	327	439	500	824	1410	1425	1888	2151	2469	2736
	4 6 0	266	308	326	457	535	949	1312	1379	1696	2241	2471	2921
	4 7 0	245	315	326	462	566	1098	1247	1357	1501	2366	2463	2764
W	4 8 0	237	318	328	462	579	1209	1237	1331	1381	2458	2460	2658
Σ	5 5 0	260	308	355	444	514	925	1294	1374	1939	1997	2615	2701
	5 6 0	241	289	375	463	539	1044	1197	1351	1754	2101	2629	2805
	5 7 0	228	274	385	475	567	1124	1193	1340	1558	2238	2610	2640
K, U	6 6 0	215	262	423	486	549	1090	1157	1338	1738	2052	2626	2757
	1 1 1	83	344	360	384	463	470	1882	1961	2190	2210	2547	2699
	1 2 1	119	332	369	395	452	481	1830	1934	2159	2245	2495	2614
	1 3 1	171	311	376	410	459	500	1747	1942	2057	2180	2497	2612
	1 4 1	214	285	379	432	506	526	1661	1903	1928	2101	2417	2677
	1 5 1	219	258	412	463	542	599	1569	1771	1802	2079	2333	2768
	1 6 1	202	236	460	496	560	746	1482	1596	1692	2089	2302	2830
	1 7 1	184	222	497	521	571	844	1405	1437	1621	2105	2297	2839
S	1 8 1	178	217	512	531	574	916	1331	1401	1597	2113	2297	2836
	2 2 1	150	333	368	398	452	492	1727	1919	2173	2347	2374	2588
	2 3 1	192	325	366	403	463	524	1630	1886	2103	2253	2475	2534
	2 4 1	227	309	356	420	501	575	1538	1829	1970	2169	2508	2593
	2 5 1	235	282	372	448	536	662	1448	1748	1809	2122	2476	2682
	2 6 1	221	258	406	479	555	787	1367	1611	1683	2118	2457	2735
	2 7 1	205	244	438	500	565	926	1308	1434	1626	2131	2455	2754
	2 8 1	199	240	453	506	568	1010	1287	1337	1607	2139	2457	2755
	3 3 1	218	338	362	398	462	574	1525	1813	2074	2319	2378	2559
	3 4 1	241	336	347	409	487	642	1429	1740	1979	2245	2410	2643
	3 5 1	254	306	347	465	521	738	1342	1669	1832	2193	2459	2754
	3 6 1	250	283	359	460	545	868	1266	1607	1650	2200	2495	2777

TABLE I. *(continued)*.

	$\vec{k}/\frac{\pi}{4a}$	Band 1	Band 2	Band 3	Band 4	Band 5	Band 6	Band 7	Band 8	Band 9	Band 10	Band 11	Band 12
	3 7 1	234	276	376	473	560	1019	1213	1458	1572	2226	2545	2713
	3 8 1	228	274	385	475	566	1124	1193	1340	1558	2239	2610	2640
	4 4 1	253	324	370	404	493	721	1334	1656	1978	2165	2449	2652
	4 5 1	265	302	364	422	516	822	1251	1586	1885	2127	2500	2719
	4 6 1	271	284	352	444	541	950	1180	1535	1702	2198	2497	2859
Q	4 7 1	252	301	339	458	559	1087	1146	1489	1523	2301	2481	2830
	5 5 1	256	300	373	429	527	918	1171	1521	1946	1982	2626	2687
	5 6 1	244	287	376	451	545	1019	1120	1480	1764	2088	2617	2806
	2 2 2	169	354	363	394	474	490	1613	1911	2277	2295	2469	2499
	2 3 2	193	357	369	390	496	516	1507	1884	2149	2314	2434	2527
	2 4 2	216	340	365	399	537	575	1409	1855	2010	2151	2578	2593
	2 5 2	229	307	375	418	556	689	1318	1783	1895	2040	2630	2650
	2 6 2	229	279	394	445	562	831	1238	1627	1809	2024	2635	2718
	2 7 2	220	266	414	472	556	986	1181	1448	1756	2042	2625	2749
U, K	2 8 2	215	262	422	486	549	1090	1157	1338	1738	2052	2626	2758
	3 3 2	200	353	382	411	498	554	1396	1846	2118	2314	2447	2492
	3 4 2	213	341	380	415	526	626	1298	1814	2011	2191	2514	2585
	3 5 2	229	317	385	411	549	740	1212	1775	1887	2089	2566	2701
	3 6 2	243	294	381	428	553	882	1143	1659	1797	2069	2596	2777
	3 7 2	244	287	376	452	545	1019	1120	1480	1764	2089	2617	2806
	4 4 2	217	333	379	437	523	702	1206	1772	1977	2152	2525	2599
	4 5 2	231	315	389	421	540	803	1135	1735	1898	2091	2549	2680
Q	4 6 2	253	292	383	421	546	909	1103	1695	1746	2126	2533	2787
	5 5 2	236	308	394	415	547	862	1099	1690	1957	1978	2630	2650
Λ	3 3 3	192	347	375	491	525	537	1285	1817	2183	2215	2510	2530
	3 4 3	197	341	371	480	550	618	1194	1798	2091	2150	2549	2564
	3 5 3	213	325	378	444	557	742	1125	1782	2004	2034	2602	2630
	3 6 3	236	308	394	415	547	862	1099	1690	1957	1978	2630	2650
	4 4 3	195	339	367	507	547	665	1123	1783	2066	2139	2556	2569
Q	4 5 3	207	330	372	468	552	744	1095	1780	1991	2088	2567	2626
L	4 4 4	188	339	365	548	562	628	1095	1774	2112	2146	2550	2558

revealed shoulders near 3 and 6 eV.

Three sets of experimental data have been selected, and the derived ϵ_2 functions are shown in Fig. 4. Curve (a), by Vehse *et al.*,[4] extends to high photon energies and was based on measurements on films *in situ*. The ϵ_2 profile presented by Johnson and Christy[11] was obtained from measurements in N_2. Weaver[27] has succeeded in reproducing these data reasonably well, and also the observation by Duisebaeva[7] [curve (c) in Fig. 3] concerning the peak at ≈0.5 has been confirmed.[27] In the same figure (Fig. 3) is a theoretical curve marked RAPW. It represents the joint density of states divided by ω^2 as calculated from the present RAPW band-structure calculation. The theoretical curve has been scaled to the experiment of Ref. 11 at 2.5 eV.

The part of the spectrum lying between 3 and 8 eV is probably the part which is most easy to relate to the band structure. Clearly the photon energy in this regime is so large that it is beyond the region where the intraband contributions can be essential, these parts being very difficult to subtract in the case of Pd where the interband transitions are important even for photon energies very close to 0. On the other hand the photon energy range 2–8 eV does not involve very-high-lying bands, and thus it covers a regime where we can have a fair confidence in the band calculation. We observe three clear changes of slope in curve (a) at A(3.0 eV), B(4.4 eV), and C(7.2 eV) which could be interband edges. Only the kink B at 4.4 eV is clearly in the experimental curve (c) as well. On the other hand, two edgelike features are seen in

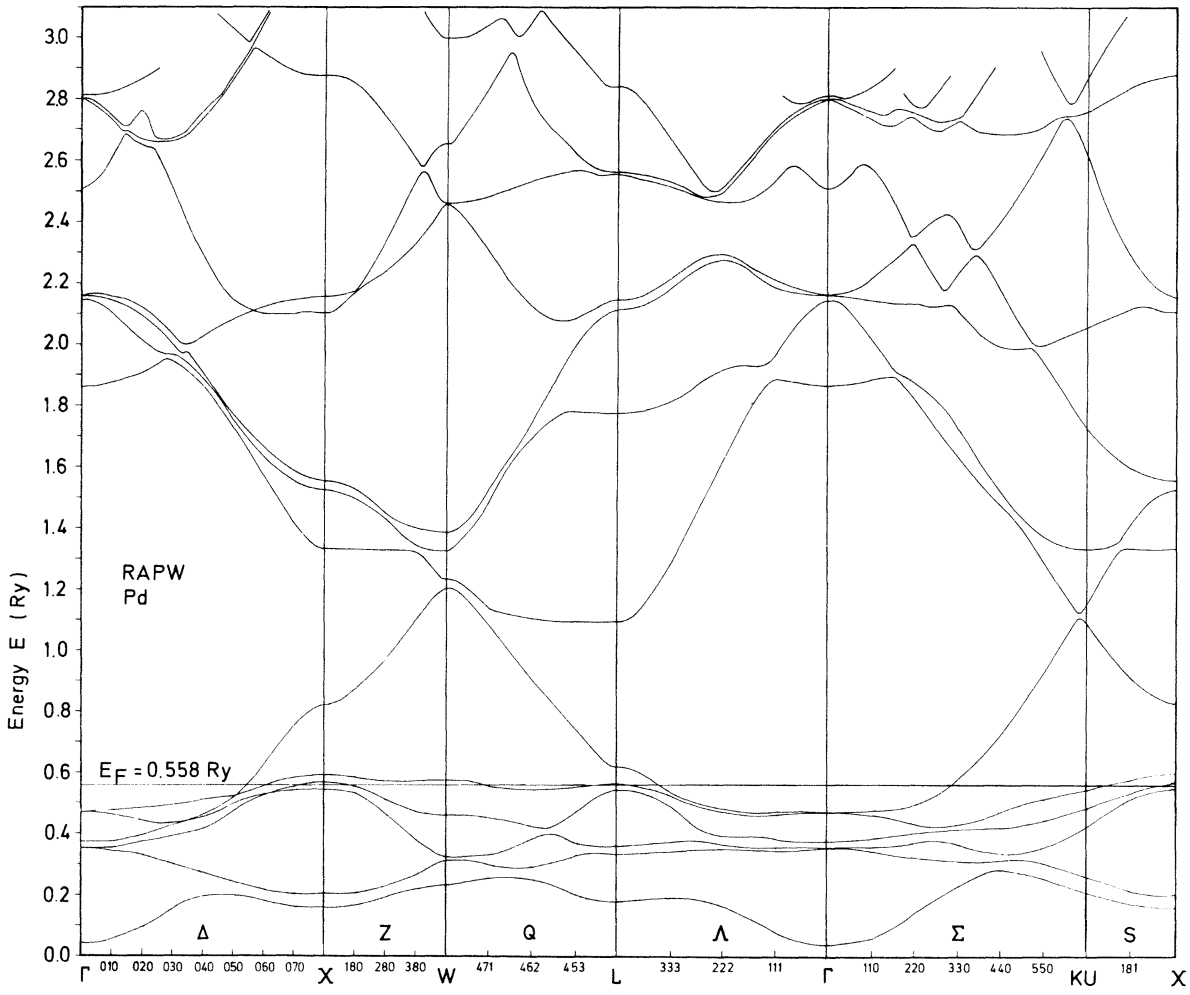

FIG. 1. Band structure of Pd along symmetry lines as calculated by the RAPW method. The fermi level $E_F = 0.558$ Ry above the muffin-tin zero.

(c) at 3.3 eV (D) and 3.7 eV (E). The kink A cannot be clearly retrieved in the theoretical trace, but B, C, D, and E all have clear counterparts in the RAPW spectrum. The big hump near B is strongly exaggerated in the theoretical curve, probably due to the assumed constancy of the matrix elements. Some information about the parts of the band structure which contribute to $\epsilon_2(\omega)$ in specific energy ranges may be obtained by examining the individual partial joint density-of-states functions $J_{if}(\hbar\omega)$ [Eq.(1)]. These functions are shown in Figs. 4(a)–4(f). It is seen that the transitions from band 3 to band 6 become essential near the spectral position A, whereas D can be related to a $2 \rightarrow 5$ edge. The onset of the $2 \rightarrow 5$ transitions at 3.3 eV takes place near and at the symmetry line Q, the final states being at the Fermi level. The $2 \rightarrow 6$ transitions are also important in this regime, but they start at somewhat lower energies. The onset is 2.94 eV (RAPW) at Λ, the final states being at E_F. The $3 \rightarrow 5$ transitions give rise to an upper edge at 3.5 eV (near W) which may be related to E. Figure 4(a) shows that J_{15} as well as J_{16} have sharp edges at 4.3–4.5 eV which could be related to B. These edges are in part due to transitions near $Q(1 \rightarrow 5)$ and $\Sigma(1 \rightarrow 6)$.

The element C at 7.2 eV in the experimental curve (a) is also found in the RAPW curve. This feature is unambiguously identified by means of the partial joint density-of-states curves [Fig. 4(e)] as representing the $5 \rightarrow 7$ edge, due to transitions from band 5 (E_F) to band 7 at the symmetry line Q. The fact that this identification appears so safe, and that the agreement between the calcula-

TABLE II. Comparison of characteristic energy separations from two *ab initio* calculations, the nonrelativistic APW calculation by Mueller *et al.* (Ref. 1) and the present RAPW calculation.

Double-group notation	Single-group notation	Band indices	Mueller *et al.* (Ref. 1) APW	Present RAPW
s bandwidth				
$X_6^- - \Gamma_6^+$	$X_4' - \Gamma_1$	6; 1	0.751	0.782
$X_6^- - L_4^-$	$X_4' - L_2'$	6; 6	0.200	0.197
$L_4^- - \Gamma_6^+$	$L_2' - \Gamma_1$	6; 1	0.551	0.585
d bandwidth				
$X_7^+ - X_6^+$	$X_5 - X_1$	5; 1	0.396	0.430
$\Gamma_8^+ - \Gamma_8^+$	$\Gamma_{12} - \Gamma_{25}'$	(6, 5); (2, 3)	0.103	0.119
$L_{6+5}^+ - L_4^+$	$L_3 - L_1$	5; 1	0.336	0.375
s-*d* separation				
$L_4^- - L_{6+5}^+$	$L_2' - L_3$	6; 5	0.133	0.066
$X_6^- - X_7^+$	$X_4' - X_5$	6; 5	0.308	0.234
"*L*-gap"				
$L_4^+ - L_4^-$	$L_1 - L_2'$	7; 6		0.467
			Ry	Ry

ted gap and the experiment is within ≈ 0.1 eV gives a strong support to the present RAPW band model since level 7 at L is particularly sensitive to the potential.

The experimental ϵ_2 function (a) has in the high-energy regime (9–25 eV) maxima near the following spectral positions, 9.7, 12.5, 15.0, 16.2, 17.3, and 20.5 eV. As follows from Fig. 3, it is extremely difficult to relate these "peaks" unambiguously to the structure in the total ϵ_2 spectrum calculated in the crude constant matrix approximation. However, considering the partial functions J_{if} in Figs. 4(c) and 4(d) it appears that the $3 \rightarrow 7$ and $4 \rightarrow 7$ transitions are contributing essentially to the 9.7-eV peak. The sharp peak in J_{47} at 9.3 eV is related to parallel-band transitions from band 4 to band 7 at a Q point. The $3 \rightarrow 7$ transitions at the symmetry point L, according to the RAPW calculation [Table I and Fig. 4(c)], give rise to a singular peak at 9.9 eV. The structure at 12.5 eV may be related to $1 \rightarrow 7$, $2 \rightarrow 7$, and $3 \rightarrow 7$ transitions. The onset of the $1 \rightarrow 7$ transitions at 12.3 eV takes place at L, whereas J_{27} has a singularity at W at $\hbar\omega = 12.5$ eV. Figure 4 shows that the only band pair which in the present model gives significant structure near $\hbar\omega = 15$ eV is $(i, f) = (1, 8)$. These transitions take place near Q and Z points, the onset (calculated to be 14.9 eV) taking place at W. Figure 4 shows that J_{58} has a very pronounced peak at $\hbar\omega = 16.8$ eV. This corresponds to transitions from band 5 at the Fermi level to band 8 in a region around L (including Q as well as Λ points). It is suggested that these transitions in the extended region around L are responsible for the structure observed at 17.3 eV in curve (a) in Fig. 3. If this interpretation is correct, one would also expect that the $4 \rightarrow 8$ peak at 18.1 eV [Fig. 4(d)] might show up in the experiment. In fact, some structure, although weak, is observed at 18.4 eV. The very obvious maximum in the experimental trace (Fig. 3) at 20.5 eV appears to coincide with a *minimum* in the calculated spectrum. However, as follows from the comments given above to the elements of structure at 17.3 and 18.4 eV we may now be considering an energy range where the RAPW calculation easily can contain errors of several tenths of an eV in magnitude. Further, what probably is more important, the constant matrix element approximation will be extremely bad in this regime since $d \rightarrow f$ transitions with high probability now can occur. According to the RAPW band calculation, the $d \rightarrow f$ transitions at Γ start near 19 eV, $(5, 6) \rightarrow 7$. The f bands in gold[28] appeared to be placed correctly by the RAPW calculation when compared to modulation spectroscopy and photoemission results, and further, the $4 \rightarrow 7$ transitions ($\Gamma_7^+ \rightarrow \Gamma_6^-$) seemed to have particularly strong transition probability. In Pd the $4 \rightarrow 7$ gap at Γ is calculated to be 20.2 eV (Table I). This value is in excellent agreement with the ex-

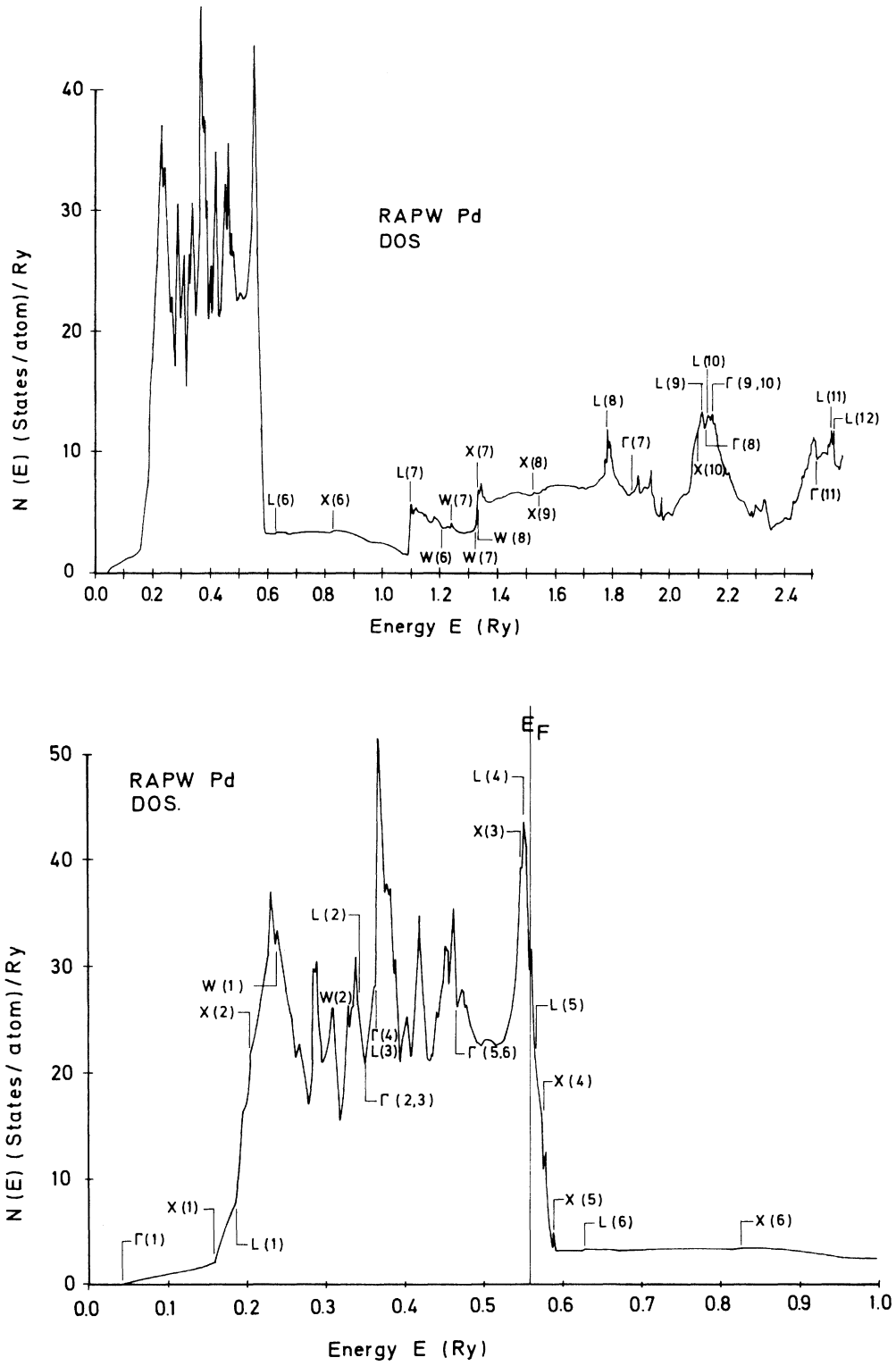

FIG. 2. (a) Density-of-states function over the entire energy range covered by the RAPW calculation. Some critical points are indicated, the numbers being the level numbers. The eigenvalues at each k point is counted from below. (b) Blowup of the DOS in the d-band range.

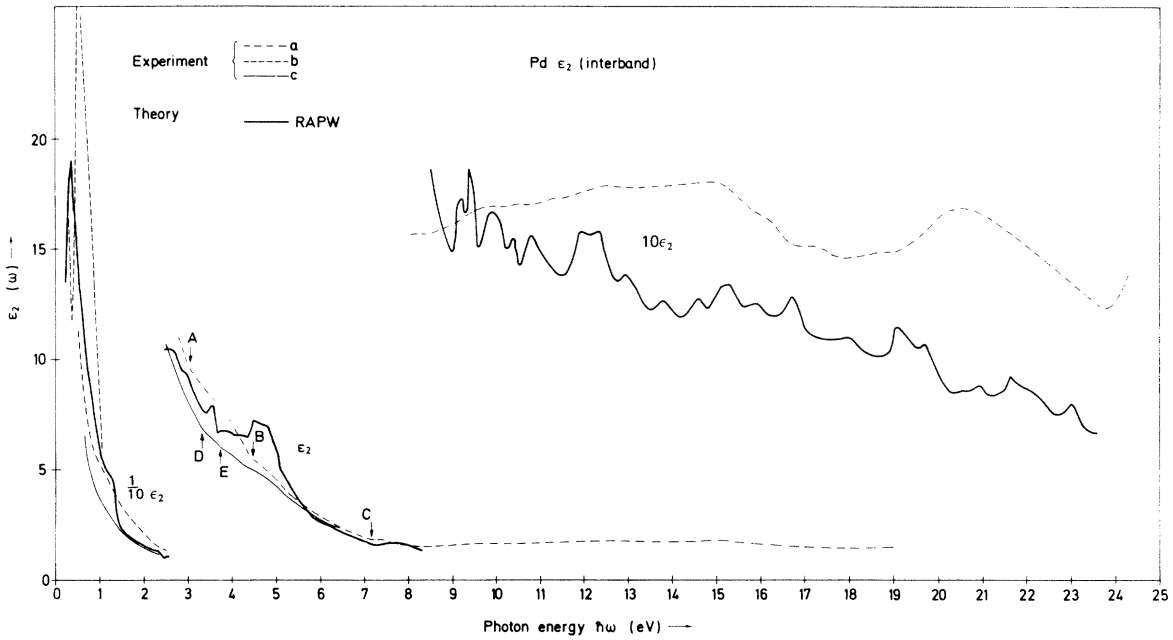

FIG. 3. Interband contribution to the imaginary part $\epsilon_2(\omega)$ of the dielectric function as calculated from the joint density of states together with experimental ϵ_2 traces. (a)–(c) Experiments by Vehse *et al.*, (a), Ref. 4, Duisebaeva *et al.* (b), Ref. 7, and Johnson and Cristy (c), Ref. 11.

periment if it is assumed to represent the edge for transitions giving rise to the broad maximum around 20.5 eV in the experimental ϵ_2 curve.[4]

In the range of low photon energies, 0–2 eV, there are large differences between the experimental results. Although the band calculation must be expected to be very good in this regime, it also follows from Fig. 3 that the theoretical ϵ_2 profile differs from the experiments. This again is ascribed to the crude constant matrix element approximation. At very low energies some d-d transitions are included in the calculation although they, due to their forbidden character, cannot be expected to contribute essentially to the spectrum. The structure which is clear in the theoretical curve at $\hbar\omega \approx 1.1$ eV may also be noticed in the experimental traces (a) and (c). Further curve (b) exhibits, as mentioned earlier, a strong peak at $\hbar\omega \approx 0.5$ eV, which also is found in the calculation. In order to analyze the optical properties further for small photon energies Weaver[27] recently performed new measurements. The results were obtained by using a high purity sample which was etched to remove work damage, annealed in vacuum to promote grain growth, then flashed in ultrahigh vacuum before it was placed in the calorimeter where the absorptivity was measured. The conductivity $\sigma(\omega)$ which was obtained after a Kramers-Kroenig analysis is shown in Fig. 5.

It follows from Fig. 5 that the new results by Weaver support the results of Duisebaeva *et al.*[7] concerning the peak at 0.5 eV, and also it is clear that a peak does sort out at 1.1 eV. It was suggested[27] that these two elements of structure essentially are due to $4 \rightarrow 5$ transitions regions around Λ and L and this is also very reasonable when compared to the present band models. The comparison to the RAPW result is obscured by the strong d-d ($3 \rightarrow 4$ near X) contribution, and therefore this has been subtracted in one of the curves shown in Fig. 5.

IV. PHOTOEMISSION

In the present analysis of the photoemission spectra of Pd, we will assume that the experimental results have been obtained from polycrystalline samples, and that "surface emission" processes[29,30] contribute negligibly to the spectra compared to bulk processes. Further, it is assumed that the bulk photoemission can be related to the one-electron band model in the manner described by the conventional three-step model, where only direct optical transitions are considered. In this model the photoelectron spectrum $N(E, \hbar\omega)$ can be expressed as

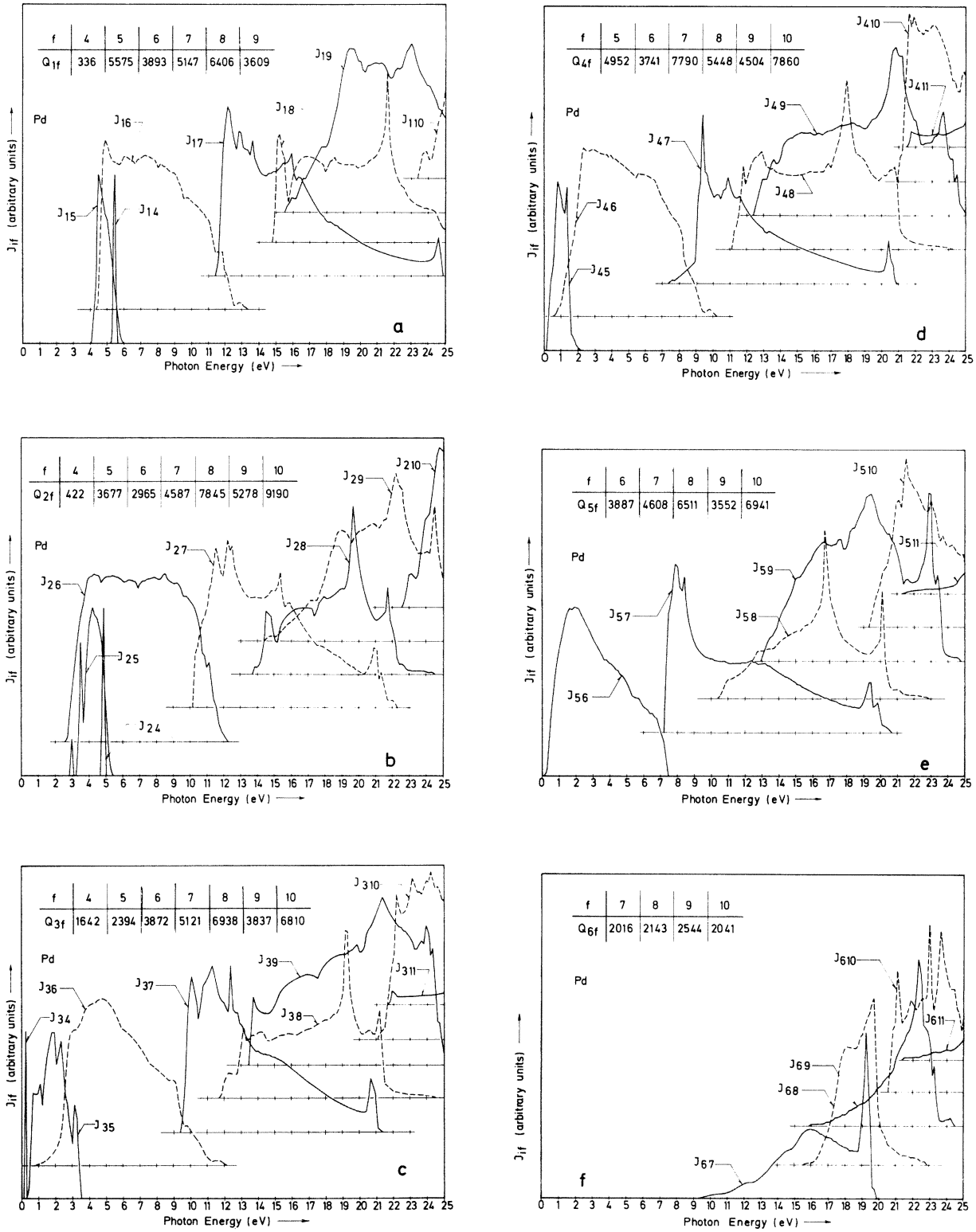

FIG. 4. (a)–(f) Partial joint density-of-states functions $J_{if}(\hbar\omega)$ as defined in Eq. (1). All functions have been scaled to the same maximum value for convenience. The numbers Q_{if} give, in arbitrary units, the maximum values, so that it is possible to estimate the relative intensities of the various J_{if} functions.

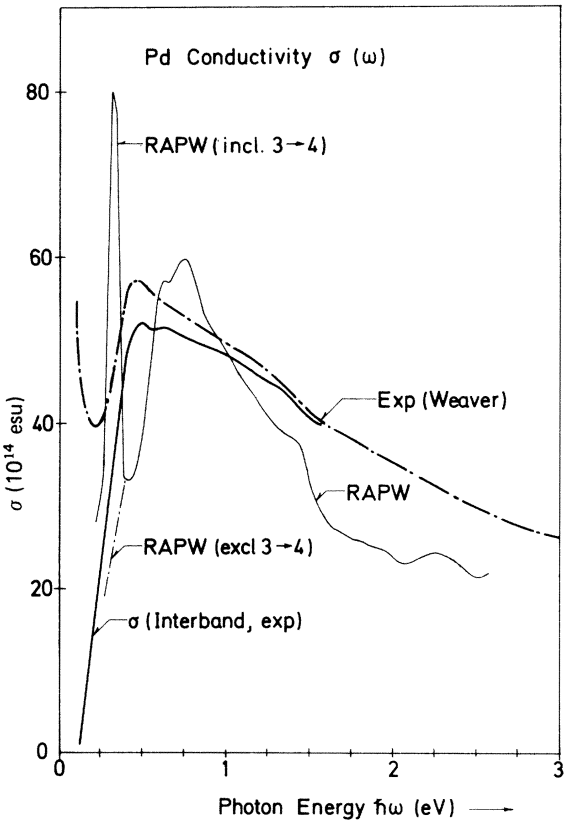

FIG. 5. Optical conductivity $\sigma(\omega)$ of palladium as measured by Weaver (Ref. 27) together with corresponding function derived from the present band-structure calculation.

$$N(E,\hbar\omega)\propto\sum_{i,f}\int d\vec{k}\,|M_{if}|^2 P(\omega,\vec{k},E_f(\vec{k}))\times\delta(E_f(\vec{k})-E_i(\vec{k})-\hbar\omega)\delta(E-E_i(\vec{k}))\times f(E_i(\vec{k}))[1-f(E_f(\vec{k}))]. \quad (3)$$

This function represents the number of electrons which are emitted when the photon energy is $\hbar\omega$ and which come from initial states with energy E. The quantity M_{if} is the momentum matrix element, whereas P is an escape function including scattering effects for the excited electrons, and to some extent their interactions with the surface. Although the model at this level is very crude, we will simplify it further. As in the case of the calculation of the optical spectra it will be assumed that the matrix elements are constant, and the function P will be replaced by an "effective" threshold function C which can be taken outside the integral in (3). The function C, which is used here, is similar to the one constructed by Berglund and Spicer,[31] and apart from a change in parameters it is identical to the function used in the calculations for silver.[26] However, the approximate escape function was derived under the assumption that the final state bands are free-electron-like which corresponds to a density-of-states function without strong singularities.

The band structure of Pd does contain critical points in the final state regime and therefore it differs significantly from the free-electron model. Excited electrons which end up at critical points will be expected to contribute little to the emission spectra since their group velocity will be vanishingly small. Therefore we include an extra factor $v_f(\vec{k})$, the final-state group speed, in the integrand of the expression for $N(E,\hbar\omega)$. Substituting the Fermi functions by step functions, our final expression for the energy distribution of emitted electrons is

$$N(E,\hbar\omega)\propto C\sum_{i,f}\int d\vec{k}\,v_f(\vec{k})\times\delta(E_f(\vec{k})-E_i(\vec{k})-\hbar\omega)\delta(E_i(\vec{k})-E), \quad (4)$$

where

$$E_i(\vec{k})\leq E_F \quad \text{and} \quad E_f(\vec{k})\geq E_F.$$

The escape function depends on the final-state energy (E_f), electron mean free path $L(E_f)$, absorption coefficient α, and the work function $e\phi$. The dependence of L on E_f was taken to be as in calculations for[32] Rh and it was adjusted to 10 Å at $E_f - E_F = 8$ eV. The dependence on α is weak, and we used $\alpha = 0.05$ Å^{-1} at all photon energies. The work function is $e\phi = 5.4$ eV. The energy distribution curves (EDC) as calculated from (4) for photon energies from 8 to 22 eV are shown in Fig. 6. The spectra have been folded by a Lorentzian of 0.5 eV FWHM (full width at half-maximum). For a rough comparison to the measurements and calculations by Janak *et al.*[17] in the photon energy range 7.7–11.6 eV we may consider our 10-eV trace as representative. This EDC is seen (Fig. 6) to have peaks at −0.2, −1.2, −2.2, and −3.6 eV. The corresponding experimental[17] peak positions are −0.15, −1.2, −2.2, and −3.5 eV demonstrating excellent agreement between the calculation and experiment with respect to spectral position of elements of structure. This agreement encourages a more detailed comparison between the calculated and measured spectra. Four photon energies, $\hbar\omega = 7.8$, 8.4, 9.4, and 10.2 eV are selected for this examination, where we compare to the measurements by Traum and Smith.[14] Figure 7 shows for $\hbar\omega = 7.8$ eV the calculated energy distribution of joint density of states (EDJDOS) [curve (a)], the calculated EDC (b), and its second derivative (c) together with three experimental traces.[14] Curve

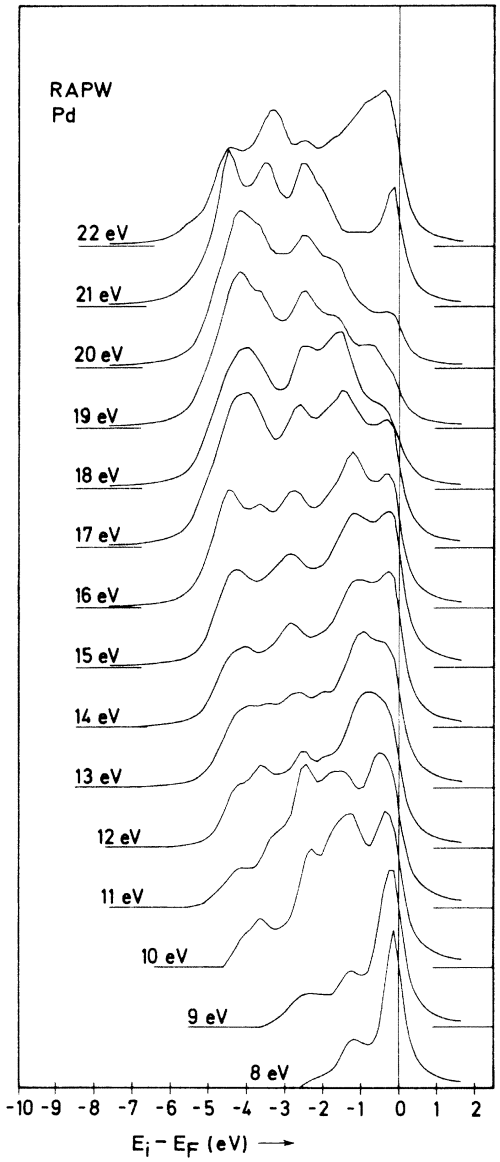

FIG. 6. Direct model energy distribution curves for Pd.

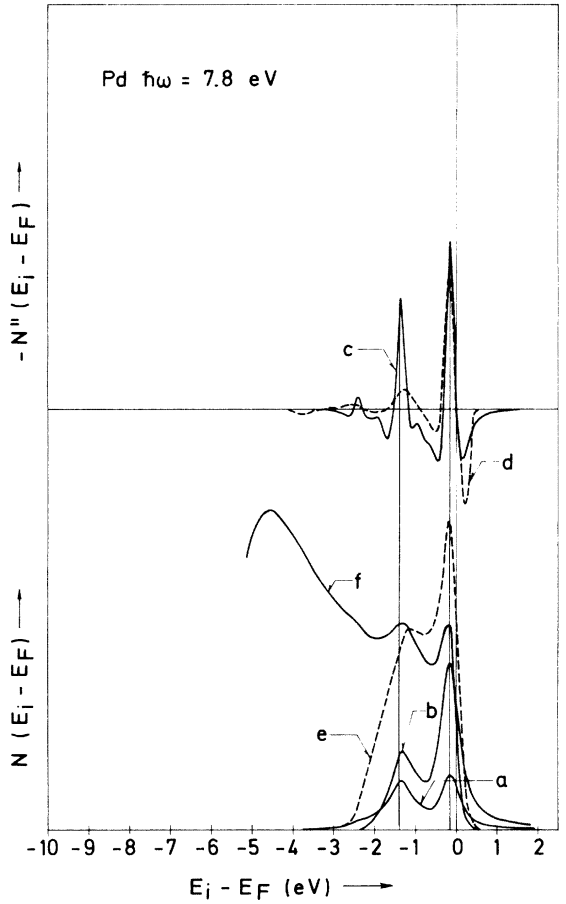

FIG. 7. Photoelectron spectra for Pd corresponding to 7.8-eV photons. (a) The calculated distribution of photoexcited electrons; (b) the calculated EDC; (c) the calculated second derivative; (e) the experimental trace (Ref. 14) obtained for a clean sample; (f) the EDC measured after cesiation; (d) the measured third harmonic of the photocurrent (Ref. 14). Vertical scales are arbitrary, and no attempt has been made to adjust amplitudes. The calculated EDJDOS and EDC functions are folded by a Lorentzian of 0.5 eV FWHM.

(e) is the EDC measured on clean Pd, whereas *f* was taken after cesiation. The curve marked (d) represents the measured second derivative of the EDC, i.e., the third harmonic of the photocurrent. There has been made no attempt to scale the amplitudes, so that the vertical scales are different, and arbitrary, for all curves. Two strong peaks are observed at −0.15 and −1.3 eV. The first one (−0.15 eV) is due to transitions from band 4 and 5 to band 7, whereas 4→6 transitions are responsible for the second peak. The spectral positions of these peaks are identical in the experimental and theoretical traces. The apparent upward shift of the second peak in curve (e) is considered as a line-shape effect due to the vacuum cutoff. A small third peak at −2.5 eV in the calculated spectra is also noticed in the spectrum taken after cesiation (f) and in the experimental second derivative (d) at −2.6 eV. This peak is due to 3→6 transitions. As will be demonstrated later, the regions in k space where the transitions corresponding to a certain peak occur may be quite extended, all three peaks discussed above at least have important contributions from k points at and close to the lines Q and Λ. An increase of the photon energy 8.4 eV (Fig. 8) produces only

minor changes in the calculated EDJDOS and EDC [(a) and (b)]. The low-lying peak has split into two as can be seen from the calculated second derivative (c). The splitting is not seen in the experiment (d), but in the 9.4-eV spectrum (Fig. 9) it can be discerned (−2.6 and −2.9 eV).

Further, at 9.4 eV the leading peak has moved down to −0.3 eV in agreement with experiment. The position of the second peak, −1.25 eV, is almost unchanged, and still matching the experiment. The calculated spectrum contains a strong peak at −1.8 eV which is not in the experimental trace, or at most it appears as a shoulder in $-N''$. The calculated peak is due to transitions from band 4 to 7 in an extremely small region around a Q point where the spin-orbit coupling produces a singularity by splitting band 3 and 4. The peak may well be exaggerated in the calculation because of slight inaccuracies in our $\vec{k}$-space interpolation leading to band extrema which are not sufficiently sharp. Also at $\hbar\omega = 10.2$ eV (Fig. 10) elements of structure appear in the calculated EDC, and in particular N'', which are not clearly present in the measured spectrum. Two such peaks in $-N''$ are found, one at −1.77 eV (3 → 7 and 4 → 7 transitions) and another at −3.1 eV. The latter is, however, very weak in the calculated EDC. The remaining elements of structure all have counterparts in the experiment and the spectral positions all agree. The calculated functions shown in the figure are broadened by 0.5 eV (FWHM). The energy positions of peaks in the unbroadened functions are (excluding the two peaks discussed above) −0.08, −0.25, −1.17, −2.33, −3.63, and −5.16 eV. All these peaks have contributions from more or less extended regions in $\vec{k}$ space. The first one (−0.08 eV) is due to 6 → 7 transitions on a circle centered at a Λ point $(1, 1, 1)(3\pi/4a)$ and 5 → 7 transitions. The regions

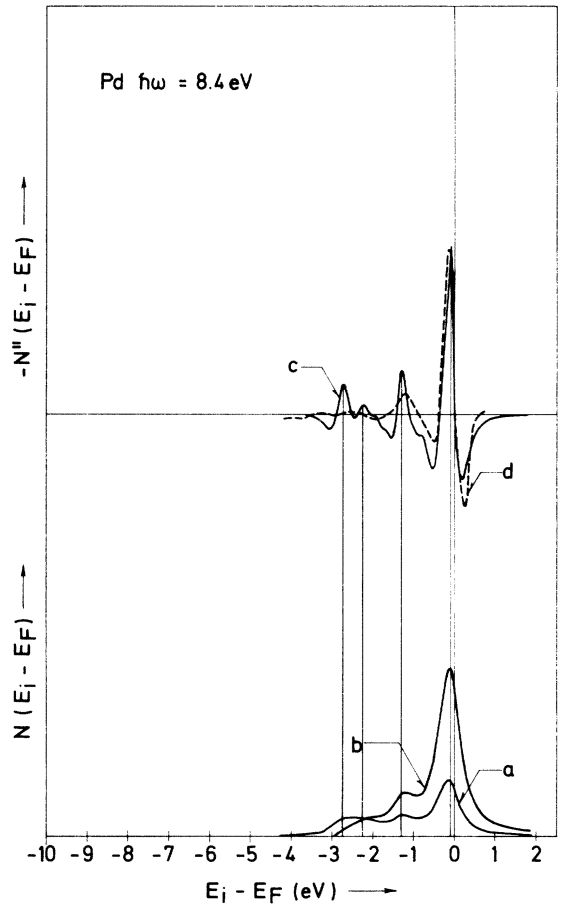

FIG. 8. Photoemission spectra for $\hbar\omega = 8.4$ eV. (a) Calculated EDJDOS; (b) calculated EDC; (c) calculated second derivative. The broken line (d) shows the experimental second derivative (Ref. 14).

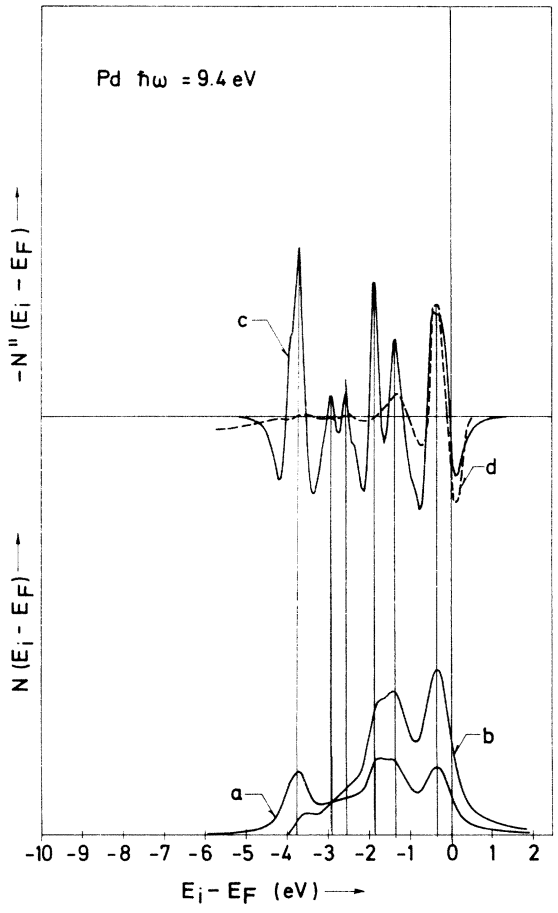

FIG. 9. Photoemission spectra at $\hbar\omega = 9.4$ eV. The signatures (a)–(d) have the same meaning as in Fig. 8.

in the Brillouin zone where the transitions occur are shown in the axiometric plot in Fig. 11. The second peak is entirely due to 5→7 transitions (Fig. 12) The seventh band also contains all the final states for the peak at −1.17 eV, the initial states being in the fourth band. The regions for these 4→7 transitions are shown in Fig. 13. The peak at −2.33 eV is very intense, and it is due to transitions over a very large region in the Brillouin zone (Fig. 14) from band 3 to band 7. The final states for the last two peaks are all in band 6. The −3.63-eV peak is due to 2→6 transitions in regions illustrated in Fig. 15, whereas 1→6 as well as 2→6 transitions contribute to the peak at −4.16 eV. The 2→6 transitions contributing to this peak are restricted to circular lines around the (1, 0, 0) axes lying in planes perpendicular to these axes close to the square zone faces (Fig. 16).

The photon energy $\hbar\omega = 10.2$ eV is particularly interesting since the calculated band structure contains two critical points, 3→7 at L and 4→7 at W with this energy gap. The initial states of these transitions are indicated in Fig. 10. It is obvious that these critical-point transitions are not placed in energy at peaks, but in this case rather where N'' is zero. The peaks in the EDC's cannot be related to transitions in specific single points, critical points, in the Brillouin zone but they have in general contributions from extended regions in $\vec{k}$ space.

V. SUMMARY AND CONCLUSIONS

The relativistic band-structure model[2] for palladium which agreed well with experiments concerning the Fermi surface has been extended to cover a large energy range and the entire Brillouin zone.

The band-structure calculation has been used in

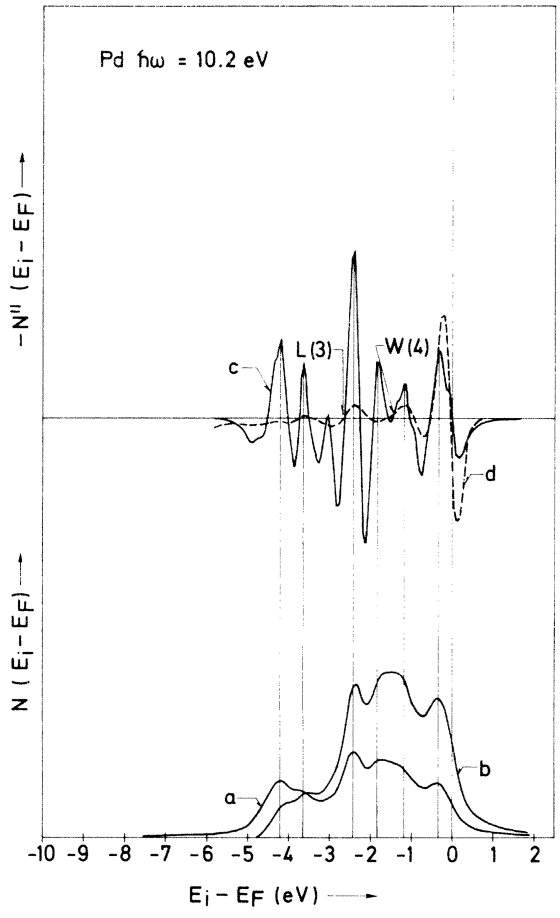

FIG. 10. Photoelectron spectra for $\hbar\omega = 10.2$ eV. The spectral positions of the initial-state energies in band 3 and 4 at L and W are indicated with arrows.

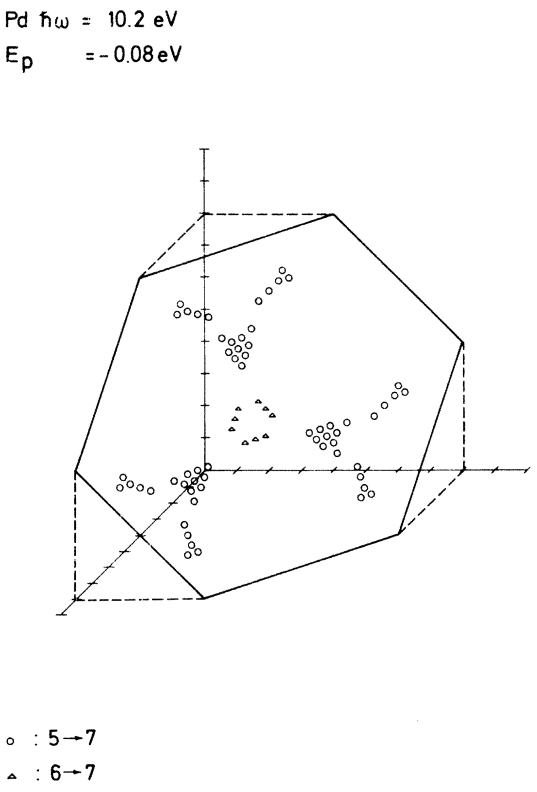

FIG. 11. Axiometric plot showing the $\vec{k}$-space regions contributing to the −0.08-eV peak in the EDC for $\hbar\omega = 10.2$ eV. The circles indicate the positions of the microcube centers from the Gilat-Raubenheimer integration where the energy of band 5 is −0.08 eV and the energy of band 7 is −0.08 eV + 10.2 eV. The triangles define in the same way the loci of 6→7 transitions.

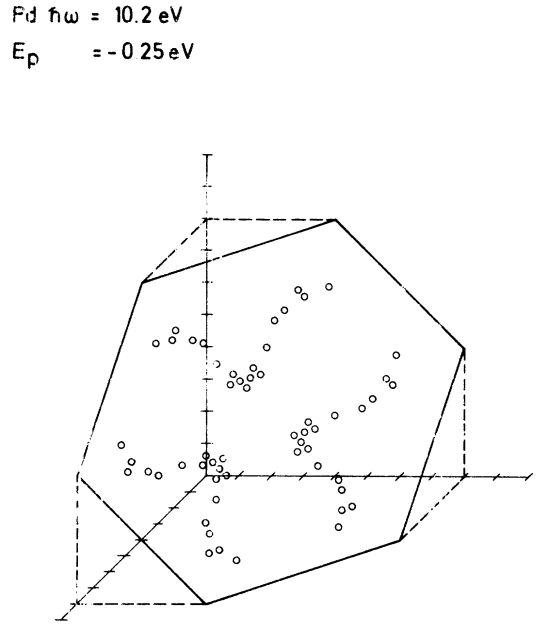

FIG. 12. Microcube centers for the transitions which take place from band 5 to band 7 and are giving rise to the peak 0.25 eV below E_F in the EDC for $\hbar\omega = 10.2$ eV.

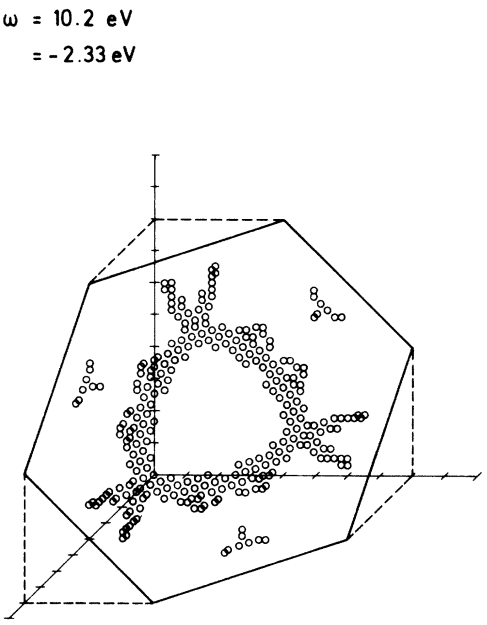

FIG. 14. Origin of the 3 → 7 transitions responsible for the peak 2.33 eV below E_F in the 10.2-eV EDC.

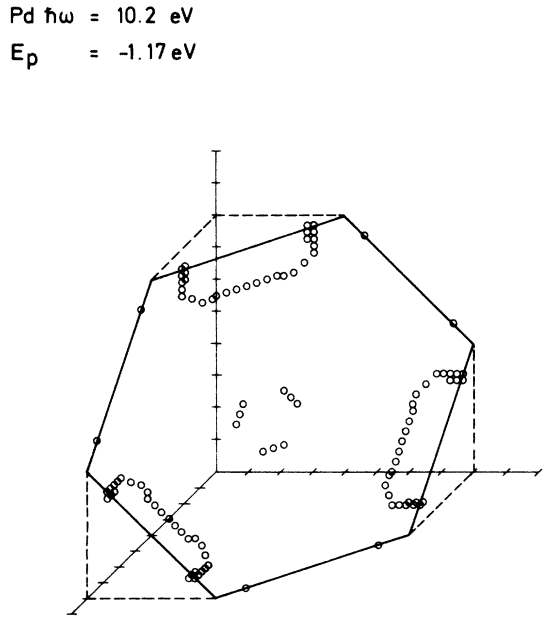

FIG. 13. Regions in $\vec{k}$ space where the transitions corresponding to the peak 1.17 eV below E_F in the 10.2-eV EDC.

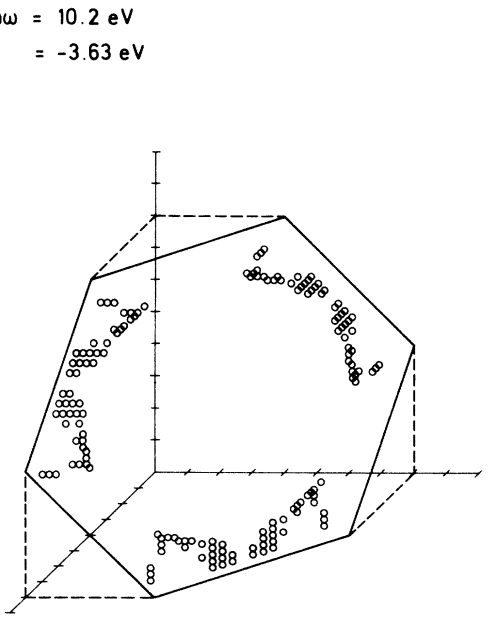

FIG. 15. Loci of 2 → 6 transitions for $\hbar\omega = 10.2$ eV having initial-state energies 3.63 eV below the Fermi level.

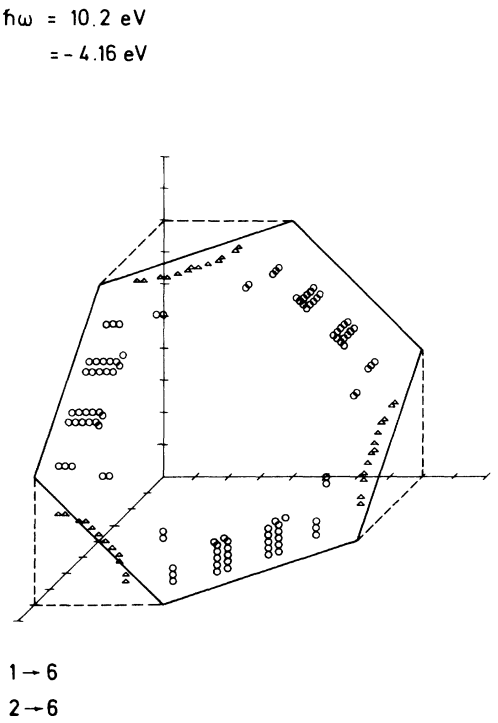

FIG. 16. Triangles indicate the loci of 2→6 transitions and circles correspond to 1→6 transitions of energy $\hbar\omega = 10.2$ eV and initial-state energy 4.16 eV below E_F.

an examination of the optical properties of Pd in the uv regime by comparing calculated ϵ_2 profiles and photoemission spectra to experimental results. The experimental $\epsilon_2(\omega)$ functions are quite difficult to obtain reliably so that independent measurements can reproduce the spectra since there are serious contamination problems. However, by comparing various experiments to our band calculation we suggest that the interband part of $\epsilon_2(\omega)$ for clean Pd should exhibit the following features. At low photon energies are two maxima at 0.5 and 1.1 eV both due to transitions from band 4 to band 5. Five edgelike features appear at 3.0, 3.3, 3.7, 4.4, and 7.2 eV corresponding to, respectively, 3→6, 2→5, 3→5, 1→5, and 5→7 transitions. The regions near L, Λ, and Q points contribute essentially. The agreement between the calculation and the experiment was particularly informative in the case of the 7.2-eV structure since we from this could conclude that the calculated value of the seventh band at L is reasonable, this level being very sensitive to the potential. Also the optical properties at high photon energies are largely influenced by the band structure around L and the lines Λ and Q. Structure at 9.7 eV is due to 4→7 transitions whereas 1→7 (around L) and 2→7 (around W) transitions are seen at $\hbar\omega \simeq 12.5$ eV. It is suggested that a maximum in the experimental trace at 15.9 eV can be related to transitions from band 1 to band 8 with an onset edge at 14.9 eV at W. The elements of structure observed at 17.3 and 18.4 eV are supposed to be due to 5→8 and 4→8 transitions. The d→f transitions at Γ start at 19.0 eV according to the RAPW calculation and the calculated $\Gamma_7^+ \rightarrow \Gamma_6^-$ gap is 20.2 eV, a value which fits the experiment nicely if it can be considered as the onset edge for transitions producing a clear maximum at 20.5 eV in the observed profile.

Also the comparison between calculation and photoemission experiments demonstrated that consistent interpretation is possible. As in the case of the optical experiments it appeared that transitions in the region around L and the symmetry lines Q and Λ play an important role. However, particular peaks in $\epsilon_2(\omega)$ as well as peaks in the EDC's cannot in general be related to transitions at singular points in the Brillouin zone, but are due to transitions in extended regions of $\vec{k}$ space.

ACKNOWLEDGMENTS

The author wants to thank J. H. Weaver for communicating unpublished results and supplying valuable information. The advice from O. K. Andersen and O. Jepsen is greatly appreciated.

[1]F. M. Mueller, A. J. Freeman, J. O. Dimmock, and A. M. Furdyna, Phys. Rev. B 1, 4617 (1970).
[2]O. K. Andersen, Phys. Rev. B 2, 883 (1970).
[3]F. M. Mueller, Phys. Rev. 153, 659 (1957).
[4]R. C. Vehse, E. T. Arakawa, and M. W. Williams, Phys. Rev. B 1, 517 (1970).
[5]A. Y.-C. Yu and W. E. Spicer, Phys. Rev. 169, 497 (1968).
[6]J. H. Weaver, Phys. Rev. B 11, 1516 (1975).
[7]Zh. Duisebaeva, M. I. Korsunskii, and G. P. Motulevich, Opt. Spektrosk. 34, 535 (1973) [Opt. Spectrosc. 34, 307 (1973)].
[8]G. A. Bolotin, M. M. Kirillova, L. V. Nomerovannaya, and M. M. Noskov, Fiz. Met. Mettalloved. 23, 463 (1967).
[9]B. Dold and R. Mecke, Optik (Stuttg.) 22, 453 (1965).
[10]P. Lostis, J. Phys. (Paris) 25, 118 (1964).
[11]P. B. Johnson and R. W. Christy, Phys. Rev. B 9, 5056 (1974).
[12]L. Hodges, H. Ehrenreich, and N. D. Lang, Phys. Rev. 152 (1966); H. Ehrenreich and L. Hodges, in *Methods in Computational Physics*, edited by B. Alder, S. Fern-

bach, and M. Rotenberg (Academic, New York, 1968), Vol. 8, p. 149.
[13]N. V. Smith and L. F. Mattheiss, Phys. Rev. B 9, 1341 (1974).
[14]M. M. Traum and N. V. Smith, Phys. Rev. B 9, 1353 (1974).
[15]N. V. Smith, Phys. Rev. B 9, 1365 (1974).
[16]N. E. Christensen, Phys. Status Solidi B 52, 241 (1972).
[17]J. F. Janak, D. E. Eastman, and A. R. Williams, Solid State Commun. 8, 271 (1970).
[18]B. Segall and F. S. Ham, in *Methods in Computational Physics* (Academic, New York, 1968), Vol. 8.
[19]D. Liberman, J. T. Waber, and D. T. Cromer, Phys. Rev. 137, A27 (1965).
[20]G. S. Painter, J. S. Faulkner, and G. M. Stocks, Phys. Rev. B 9, 2448 (1974).
[21]N. E. Christensen and B. O. Seraphin, Phys. Rev. B 4, 3321 (1971).
[22]G. Gilat and L. J. Raubenheimer, Phys. Rev. 144, 390 (1966).
[23]F. Herman and S. Skillman, *Atomic Structure Calculations* (Prentice-Hall, Englewood Cliffs, N. J., 1963).
[24]D. B. B. Rijsenbrij and J. M. Fondse, Solid State Commun. 17, 1081 (1975).
[25]N. E. Christensen, Phys. Status Solidi 31, 635 (1969).
[26]N. E. Christensen, Phys. Status Solidi B 54, 551 (1972).
[27]J. H. Weaver (private communication).
[28]N. E. Christensen, Phys. Rev. B 13, 2698 (1976).
[29]N. E. Christensen and B. Feuerbacher, Phys. Rev. B 10, 2349 (1975).
[30]B. Feuerbacher and N. E. Christensen, Phys. Rev. B 10, 2373 (1975).
[31]C. N. Berglund and W. E. Spicer, Phys. Rev. 136, A1030 (1964).
[32]N. E. Christensen, Phys. Status Solidi 55, 117 (1973).